2018

Development And Practical Application Of A Natural Gas Expansion Turbine For Power Generation Without Additional Heating Equipment

Hanushan Vasuthevan
Chair of Fluidics, TU Dortmund University, Germany, hanushan.vasuthevan@tu-dortmund.de

Andreas Bruemmer
TU Dortmund University, Germany, andreas.bruemmer@tu-dortmund.de

Christian Badura
Innogy SE, Germany, christian.badura@innogy.com

Development and Practical Application of a Natural Gas Expansion Turbine for Power Generation Without Additional Heating Equipment

Hanushan VASUTHEVAN[1]*, Andreas BRÜMMER[2], Christian BADURA[3]

[1]TU Dortmund University, Chair of Fluidics,
Dortmund, Germany
Phone: +49 231 755 5723, Fax: +49 231 755 5722, E-mail: hanushan.vasuthevan@tu-dortmund.de

[2]TU Dortmund University, Chair of Fluidics,
Dortmund, Germany
Phone: +49 231 755 5720, Fax: +49 231 755 5722, E-mail: andreas.brümmer@tu-dortmund.de

[3]Innogy SE
Essen, Germany
Phone: +49 201 12 29337, E-mail: christian.badura@innogy.de

* Corresponding Author

ABSTRACT

The efficient transportation of natural gas takes place in a high pressure state before it is distributed to the consumer at lower pressure. Generally, pressure reduction in gas grids is realized in pressure control stations with a regulating valve, where the dissipative energy remains as heat in the fluid. Nevertheless, the gas temperature decreases during the pressure reduction due to the Joule-Thomson-Effect, the magnitude depending on pressure change across the regulating valve. For higher pressure differences, it is necessary to preheat the natural gas to prevent condensate formation and freezing of pipelines. Instead of using a regulating valve, an expansion machine can be used for pressure reduction and power generation apart from pressure control stations. For this purpose, a single stage axial flow turbine is developed for power generation in a natural gas pipeline. The "preheating" of natural gas is realized solely with geothermal energy out of the upper layer of earth and thus without additional heating equipment. The temperature of natural gas at the inlet of the expansion machine is given by the temperature of the ground providing geothermal energy, typically T_{in} = 278 - 283 K. The expansion turbine outlet temperature should not fall below a level of about T_{out} = 273 K. The design criterion for the expansion machine is, therefore, the temperature difference, not the pressure difference as is common for expansion processes. Design of an axial flow impulse turbine for this application is carried out using mean diameter calculations. Losses are predicted for blade rows using empirical models. The axial flow turbine is designed in a compact module (generator inside the pipeline) for a natural gas pipeline with relevant safety standards. A first prototype of a single stage axial turbine with partial admission is manufactured and tested in a natural gas pressure control station. Results from field measurements and simulation are compared and analyzed with respect to the operational behavior of this new concept of an axial turbine for natural gas without preheating equipment.

1. INTRODUCTION

Natural gas is a mixture of flammable gases, primarily methane. The main use of natural gas as a fossil fuel is e.g. heating of rooms, providing heat for thermal processes in industry, and for electrical power generation. Generally, the transportation of natural gas after extraction is realized in long distance pipeline systems. Main components of this system are pipelines, gas compressor stations, and underground storage facilities. Gas compressor stations keep the pressure in the pipelines at a high level - approximately 8 MPa for efficient transportation. Furthermore, compressor stations are needed to temporarily store natural gas in underground facilities. Before natural gas is supplied through distribution networks to the final consumers, the pressure is reduced in pressure regulation and distribution stations,

this typically by means of pressure reduction valves. During this process, temperature drops depending on the pressure reduction which is approximately 0.5 K /0.1 MPa for an isenthalpic throttling process across the valve. Therefore, natural gas is preheated before the pressure is reduced to avoid condensation of water within the pipe and condensation of humid air outside of the pipe. These effects can lead to corrosion, freezing and blocking of pipes and valves. The potential of the pressure difference between natural gas transport systems and the distribution systems provides an opportunity to apply an expansion machine for electricity generation. Expansion machines in pressure regulation stations exist in some pressure regulation stations e.g. in Dortmund (Ger), Wetzlar (Ger), Arlesheim (CH), and Oberbuchsiten (CH). In these systems, a high pressure drop over the expansion machine is realized. Therefore, the natural gas is preheated by means of heat exchanger in the pressure regulation station. Furthermore, these systems are characterized by significant restructuring of the regulation stations requiring high investment costs. Restructering of a large number of pressure regulation stations is not economically viable due to space requirements requiring major rearrangement in the station, rebuild work on the systems, and due to high operating costs (e.g. maintenance).
In this paper the development and the practical application of a single stage axial flow impulse turbine with partial admission for a pressure regulation station is shown. The system operates without additional equipment for preheating the gas. In this approach, gas is heated solely by means of geothermal energy. The initial concept is based essentially on underground pipelines. The gas temperature is close to the temperature below the surface, T_{bs} = 283 K. With this as the system inlet temperature, gas flows through the axial turbine while pressure and temperature drop. The turbine is designed in such a way that the outlet temperature T_{out} does not fall below a minimum, typically T_{min} = 273 K. After expansion, the gas is reheated to a level near that of the surroundings by means of geothermal energy. Subsequently, natural gas can flow through the next expansion machine and the process can be repeated several times until the pressure at the outlet of the expansion system has been reduced to the target level. Figure 1 shows a qualitative example of how temperature and pressure might progress over a pipeline with expansion machines below the surface. An expansion machine for a pressure regulation station, where the inlet and outlet pipelines of the station lie below the surface has been designed and built. Due to the low available temperature difference or rather low enthalpy difference, essential criteria for the whole concept is a simplified integration in a pipeline and an economical solution for the electricity generation module. The averaged normal volume flow of the pressure regulation station is low (400 Nm³/h), thus the expected electrical power is low as well. Nevertheless, the station chosen for this work serves as a suitable experimental facility for testing purposes.

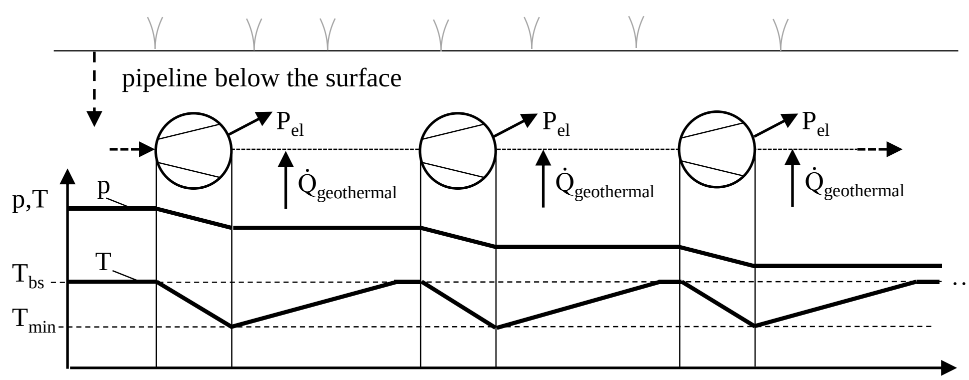

Figure 1: Qualitative temperature profile and pressure profile along a pipeline with expansion machines

2. THERMODYNAMIC POTENTIAL

The thermodynamic potential can be calculated using the enthalpy difference between the inlet h_{in} and outlet h_{out} of the expansion process shown in an hs – diagram for natural gas (Figure 2). The available potential, which can be used without preheating, is shown here for an expansion from the isothermal curve T_{in} = 283 K to the isothermal curve T_{out} = 273 K at different inlet pressures. The expansion is shown here for isentropic and irreversible process, whereby the internal isentropic efficiency is given in Equation (1). It should be noted, that the state of the actual outlet enthalpy h_{out} and isentropic outlet total enthalpy $h_{out,s}$ are related to the same outlet pressure p_{out}.

$$\eta_{i,s} = \frac{h_{in} - h_{out}}{h_{in} - h_{out,s}} \tag{1}$$

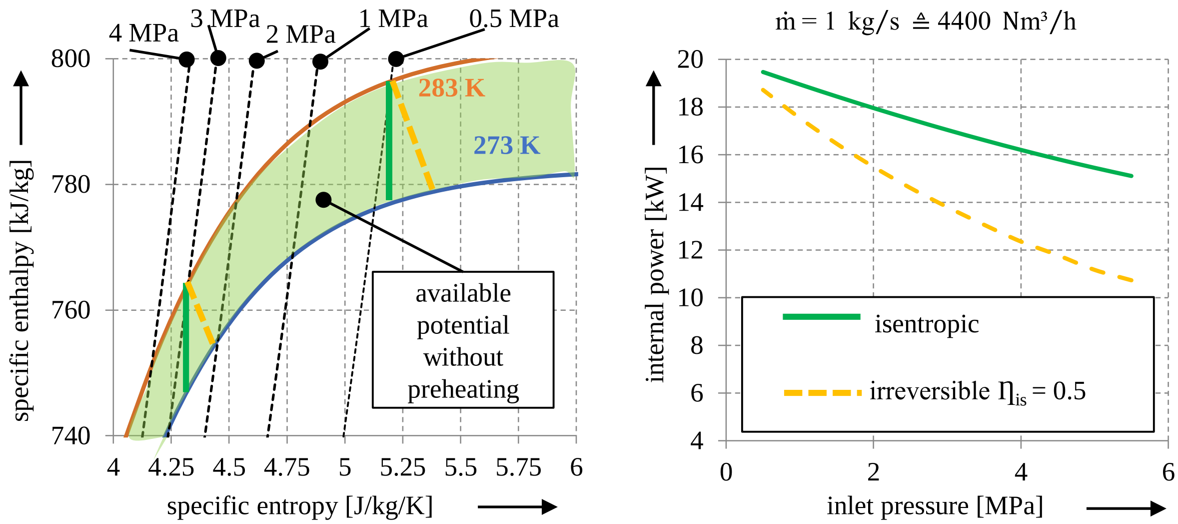

Figure 2: Left:hs – diagram of natural gas with available potential without preheating. Right: internal power over inlet pressure for a mass flow of 1 kg/s natural gas

For lower pressures, the difference between the isentropic and irreversible expansion process is small for the same temperature difference between inlet and outlet; this is due to the almost horizontal nature of the isothermal curves. The disadvantage of a poor internal isentropic efficiency is that the outlet pressure will be less than for an isentropic process but the specific enthalpy difference will remain almost constant. This effect will be more significant in the higher pressure range as shown in Figure 2. Here, the internal power over the inlet pressure is shown for a natural gas mass flow of 1 kg/s. For increasing inlet pressure, the gap between the irreversible internal power curve and the isentropic curve is widening. Furthermore, it can be seen that the actual thermodynamic potential for the isentropic process decreases at higher pressures.

3. SIMULATION PROCEDURE AND MODELLING OF AXIAL TURBINE STAGE

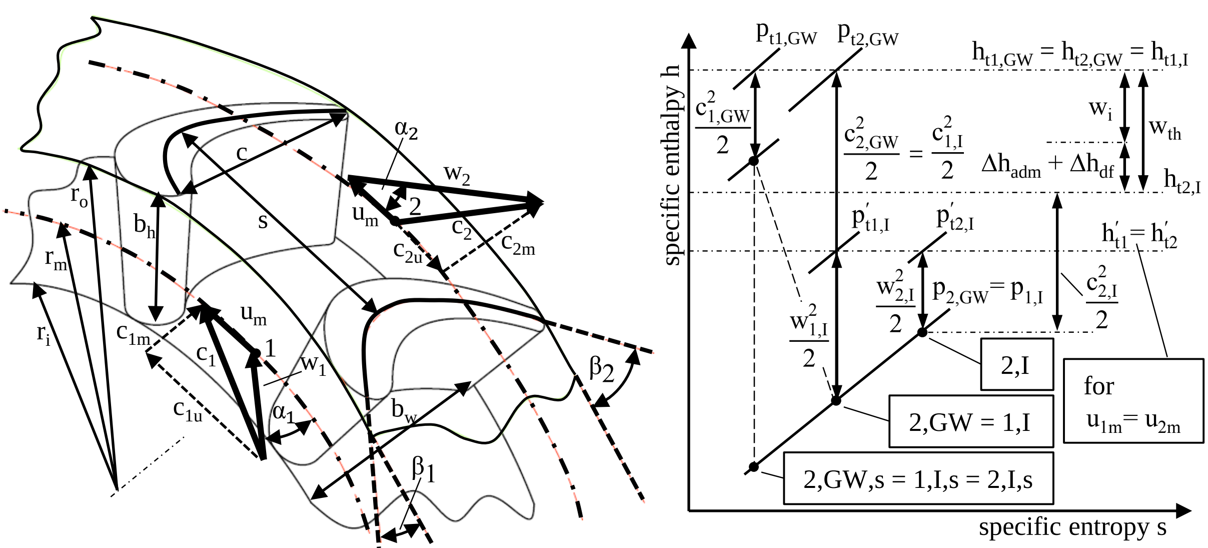

Figure 3: Left: Flow passage of a blade row with geometrical parameters and velocity triangles. Right: change of state for an impulse stage in an hs – diagram

This chapter describes the approach for the thermodynamic and fluid mechanic design of an axial turbine stage. The approach is illustrated in Figure 3, showing a typical blade row flowpath and an hs – diagram for an axial impulse turbine stage. This figure will serve as a reference for the discussion in the remainder of this chapter. The design is based on one dimensional flow models applied at mean radius r_m combined with empirical models for calculation of two – and three – dimensional losses in blade rows. Calculations are performed for the guide wheel, GW, and the impeller, I, from the inlet of a blade row (point 1) to the outlet of a blade row (point 2). The simulation tool is coupled with REFPROP (Lemmon 2013) to calculate fluid state variables. The essential aim of the calculation is to predict the specific internal work of the turbine for given boundary conditions. The theoretical specific work can be calculated with Euler's turbine equation (Equation 2) by means of the velocity triangle at the inlet and outlet of the impeller, where the circumferential speed u_m is evaluated at the mean radius and is equal at the inlet and outlet due to the selection of constant outer radius and blade height through the turbine. The difference between the specific theoretical work w_{th} and the specific internal work w_i is that the specific internal work considers disk friction and partial admission losses.

$$P_{th} = \dot{m} w_{th} = \dot{m}\left(c_{1u} u_m - c_{2u} u_m\right) \tag{2}$$

The essential steps of the simulation procedure are the initial calculation of thermodynamic states, velocities, and flow angles at the inlet and outlet of the guide wheel and impeller for given input parameters. With the results of the initial calculation, optimal blade row geometry is calculated for the guide wheel and the impeller. Subsequently, losses for the blade rows can be calculated by means of empirical models, where the actual specific internal work and the internal power can be determined.

3.1 Input Parameters

For the beginning of the simulation, the following geometric parameters are required for the guide wheel and impeller: outer radius r_o, blade height b_h, axial blade width b_w and radial clearance heights between casing and blades h_c. Furthermore, the inlet blade angle $\beta_{1,GW}$ and $\beta_{2,GW}$ of the guide wheel are required. In addition, the polytropic degree of reaction, defined in Equation (3), must be pre-determined. For an impulse stage, the degree of reaction is approximately $r_p = 0$, which means that there is no change in pressure between the impeller inlet and outlet.

$$r_p = \frac{\int_{1,I}^{2,I} v dp}{\int_{1,GW}^{2,I} v dp} \tag{3}$$

The boundary conditions for the turbine stage are: design normal volume flow, inlet pressure, inlet temperature, outlet temperature, and rotational speed. In addition, the blade row efficiency for the guide wheel is estimated. The guide wheel efficiency is the static enthalpy difference referred to the isentropic static enthalpy difference between inlet and outlet of the guide wheel. Furthermore the internal isentropic efficiency (Equation 1) is estimated for the initial calculation.

3.2 Initial Calculation

The thermodynamic variable states, velocities, and flow angles are calculated with all the input parameters given above to fulfill the boundary condition. The calculations are based on the one-dimensional conservation of mass and energy for steady state and adiabatic flow, which are given in Equation (4) – (6).

mass
$$\dot{m}_1 = \dot{m}_2 = c_{1m}\rho_1\left(p_1, T_1\right)A_1 = c_{2m}\rho_2\left(p_2, T_2\right)A_2 \tag{4}$$

energy - guide wheel
$$h_{t1,GW} = h_{t2,GW} = h_{1,GW}\left(p_{1,GW}, T_{1,GW}\right) + \frac{c_{1,GW}^2}{2} = h_{2,GW}\left(p_{2,GW}, T_{2,GW}\right) + \frac{c_{2,GW}^2}{2} \tag{5}$$

energy - impeller
$$h_{t1,I}^* = h_{t2,I}^* = h_{1,I}\left(p_{1,I}, T_{1,I}\right) + \frac{w_1^2}{2} - \frac{u_m^2}{2} = h_{2,I}\left(p_{2,I}, T_{2,I}\right) + \frac{w_2^2}{2} - \frac{u_m^2}{2} \tag{6}$$

The mass flow is constant over the turbine stage for the steady state flow and is dependent on meridian velocity, density, and area. It should be noted that only the flow area at the inlet of the guide wheel can be influenced. The flow area at the outlet of the guide wheel, and at the inlet and outlet of the impeller are assumed to be the same, a result fulfilling the boundary conditions. Based on conservation of energy, it can be derived that total enthalpy h_t through a stationary blade row remains constant and that rothalpy h_t^* stays constant through a rotating blade row, where w is the relative velocity. For constant circumferential speed, the specific relative total enthalpy $h_t^{'}$ stays also constant.

3.3 Calculation of Blade Row Geometry

The approach by Aungier (2005) is chosen for determination of blade row geometry. In the following, only the essential geometric parameters are presented. For a detailed view, refer to Aungier (2005).
On the basis of the flow field from the initial calculation, blade row details are created for the guide wheel and impeller. The essential parameters are blade angles and pitch-to-chord s/c ratio of each blade row. The inlet blade angle of a blade row is determined as the inlet flow angle. For the outlet flow angle, there is a deviation between the fluid flow angle and the blade angle; this deviation depends on the velocities and the blade angles. Deviation can be taken into account for the blade angle in such a way that the flow angle from the initial calculation is still ensured. The pitch-to-chord ratio is an essential parameter for the total pressure losses of the blade row and is chosen in such a way that the total pressure loss is minimized.

3.4 Recalculation with Losses of Blade Rows

With the determination of blade rows, more detailed information about the geometry is available and an accurate analysis of the specific internal work is possible. This is accomplished using total pressure loss coefficients. The calculation of the coefficients uses empirical models which are based entirely on Aungier (2005). Aungier (2005) refers to empirical models developed from Ainley and Mathieson (1950), Dunham and Came (1970), and Kacker and Okapuu (1981), these presented with modifications and improvements. In Equations (7) and (8), the total pressure loss coefficient of the blade row and the definition of the total pressure for compressible fluids is shown for guide wheel and impeller.

guide wheel
$$Y_{t,GW} = \frac{p_{t1,GW} - p_{t2,GW}}{p_{t2,GW} - p_{2,GW}} \; ; \; p_{t,GW} = p_{GW}\left[1+\left(\frac{\kappa-1}{2}\right)Ma^2\right]^{\frac{\kappa}{\kappa-1}} \tag{7}$$

impeller
$$Y_{t,I} = \frac{p'_{t1,I} - p'_{t2,I}}{p'_{t2,I} - p_{2,I}} \; ; \; p'_{t,I} = p_{I}\left[1+\left(\frac{\kappa-1}{2}\right)Ma_{\mathrm{Rel}}{}^2\right]^{\frac{\kappa}{\kappa-1}} \tag{8}$$

In the following the loss mechanisms consider as part of the total pressure loss coefficient of a blade row are listed without giving any detailed description:

profile loss coefficient	Y_P
secondary flow loss coefficient	Y_S
blade clearance loss coefficient	Y_{CL}
trailing edge loss coefficient	Y_{TE}
shock loss coefficient	Y_{SH}
blade row loss coefficient	$Y_t = Y_P + Y_S + Y_{CL} + Y_{TE} + Y_{SH}$

The total pressure loss coefficient of a blade row is the sum of the individual loss coefficients. With the total pressure loss coefficients and conversation of mass and energy, variables of state point fluid properties, velocities, and flow angles can be calculated again to fulfill the boundary conditions. The change in the flow field also changes the total pressure loss coefficients. Thus, the recalculation is repeated until the calculated flow field and the total pressure loss coefficients remain constant. Subsequently, the internal power is calculated with consideration of parasitic losses, which do not affect total pressure loss, but do result in an increase of the specific total enthalpy at the outlet of the turbine. These parasitic losses, described by Aungier (2005), are:

partial admission loss	Δh_{adm}
disk friction loss	Δh_{df}
specific total enthalpy – outlet	$h_{t,out} = h_{t2,I} + \Delta h_{adm} + \Delta h_{df}$

The consideration of losses by empirical models replaces the estimation of the isentropic efficiencies from the initial calculation. The last step is the comparison of internal isentropic efficiency with the estimated internal isentropic efficiency. If the calculated efficiency and the estimated efficiency are not the same (within a tolerance), the whole calculation is repeated, starting from the initial calculation with the new calculated internal efficiency from the recalculation as the new estimation. This is performed until the new calculated efficiency does not change anymore.

4. BOUNDARY CONDITION, DESIGN AND PRACTICAL APPLICATION

This Chapter first describes the boundary condition for the design of the turbine. Subsequently, the design of the single stage axial flow impulse turbine with partial admission will be presented. Finally, the practical application in a pressure regulation station is explained.

4.1 Boundary Condition

The pressure regulation station chosen for testing purposes is called "Balve - Hoennetal (Germany)", which is the last station before natural gas is supplied to private households. Boundary conditions for the pressure regulation station are shown in Table 1. In this station, gas pressure is reduced from 0.8 MPa to 0.13 MPa by means of a regulation valve. The pressure reduction valve measures the pressure at the outlet of the station and regulates the opening of the valve, thus maintaining a constant pressure at the outlet. Inlet gas heating equipment is not installed in this station, due to the low pressure reduction through the valve.

Table 1: Boundary condition of pressure regulation station

inlet pressure of station	$p_{in,st}$	0.8	MPa
outlet pressure of station	$p_{out,st}$	0.13	MPa
mean normal volume flow (load profile of a year)	$\dot{V}$	400	Nm^3/h

The turbine is planned to be installed between the pressure reduction valve and the outlet of the pressure station, which means that the pressure of 0.13 MPa downstream the turbine is held constant by the reduction valve. Thus, the inlet pressure of the turbine varies depending on the volume flow. The boundary conditions for design of the turbine are: normal volume flow of 400 Nm^3/s, inlet temperature of 283 K, temperature difference of 10 K, and outlet pressure of 0.13 MPa. For these boundary conditions, a performance analysis is carried out. Some essential results of the selected geometric parameters are presented in Table 2. The predicted performance will be presented in chapter 5 and will be compared with experimental results.

Table 2: Essential geometric parameters of axial turbine stage

	guide wheel	**impeller**	
nominal diameter DN	400	400	-
blade height	20	20	mm
blade width	50	15	mm
radial clearance	0.05	0.2	mm
blade angle inlet/outlet	90/15	20/20	°
blade shape	venturi nozzle	symmetric - impulse	-
number of blades	5	110	-
pitch-to-chord ratio	0.2	0.74	-

4.2 Design

For an economical solution, it was a requirement that the whole turbine module be installed in a pipe with constant diameter. Figure 4 shows an exploded view of the partial admission axial turbine. The generator is free hanging on the carrier flange in the gas flow. The generator wiring feeding electrical energy into the supply grid can be brought out of the pipe through the gas-tight cable gland. The nozzle is mounted on the carrier flange where natural gas is accelerated and directed partially to the impeller. The impeller is behind the carrier flange coupled directly on to the generator shaft, which extends through the middle hole of the carrier flange. A flow straightener is installed downstream of the impeller to minimize the vortex flow after the impeller. This is only necessary in case important measurement or regulation devices are arranged downstream of the turbine.

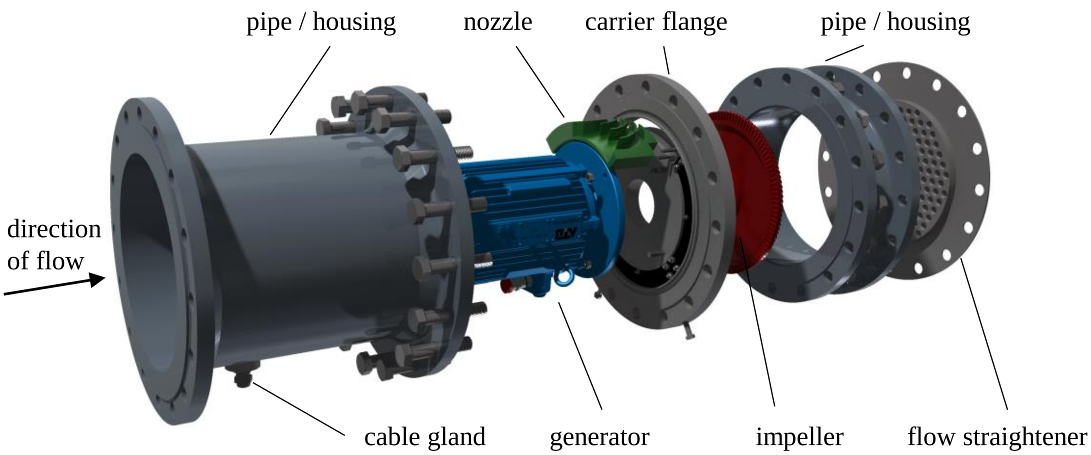

Figure 4: Exploded assembly view of the axial flow turbine with partial admission

The turbine was manufactured in the mechanical workshop at the TU Dortmund University. Nozzle and impeller, shown in Figure 5, are made from aluminum. The impeller was dynamically balanced with a balance quality of G 2.5 at 6000 rpm.

Figure 5: Left: Nozzle Right: Impeller

4.1 Practical Application in A Pressure Regulation Station

Figure 6 shows the original regulation station layout (left) and the station fitted with the experimental turbine (right). The station has of a main and a reserve line; both have a turbine flowmeter, pressure regulation valve (not shown), and filter (not shown). After filtering, pressure reduction and metering of volume flow, natural gas flows from the outlet through the pipe below the surface; arrows mark the flow route.
The turbine was arranged under the pipe bridge, which was used as a bypass. The turbine can be isolated completely from the regulation station by means of valves, thus natural gas can flow through the bypass to the outlet. Measuring points are marked with circles. Pressure and temperature at the outlet and the inlet of the turbine are measured. Furthermore, the temperature immediately behind the impeller and the acceleration to analyze vibration at the carrier flange are measured. The pressure at the outlet, which is held constant at 0.13 MPa, is the measuring point for the pressure reduction valve. The pressure at the turbine inlet is varied depending on volume flow.
Nominal power of the asynchronous motor used as a generator is 7 kW and the maximum rotational speed is 6000 rpm. Furthermore, the generator is equipped with an electromagnetically pre-stressed mechanical brake. The release of the brake can only be performed with electrical power supply. This is a safety feature to prevent operation of the turbine without load at high rotational speeds in the event of a power grid failure. The electrical energy is fed to the electrical grid over a cable, which is brought out the pipe by means of a gas-proof cable gland. The control cabinet is located in a room behind the turbine unit. This space is a non-Ex-zone in contrast to the room of the turbine. Essential parts of the control unit are a frequency converter, a PLC, and a data transfer device. A frequency converter allows electrical current to be fed into the electrical grid with 50 Hz alternating voltage. The PLC controls the temperature at the outlet of the regulation station and regulates the rotational speed of the turbine in order to control the outlet temperature. As long as the outlet temperature is in the acceptable range, rotational speed is adjusted to the maximum electrical power output, this being is measured by the frequency converter. The data transfer device forwards all measurements (averaged over three minutes) and status of the turbine to a central location for monitoring purposes. Furthermore, the turbine can be shut down remotely in the event of disturbances. The turbine has been in operation

since 2016 and is used primarily in the period from September to April, where the volume flow is high enough for a reasonable use. Volume flow depends mainly on the demand from the private households, which is higher in the winter month due to heating requirements.

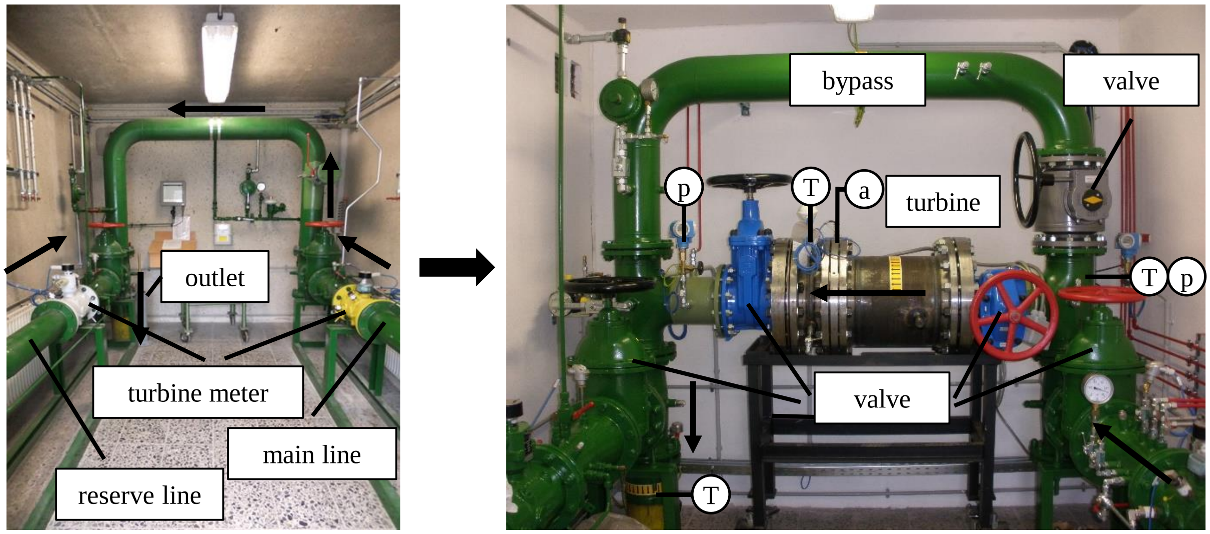

Figure 6: Left: Initial situation of pressure regulation station. Right: Final situation with axial flow turbine

5. EXPERIMENTAL RESULTS

In the following information acquired from the data transfer device is compared with simulation results. As noted in the previous section, experimental results are averaged over three minutes. Within time span, volume flow and rotational speed can change. A typical normal volume flow profile over the time for a typical day is shown in Figure 7. It can be seen that the volume flow is continuously fluctuating, thus it seems inappropriate to compare a time averaged value over three minutes with simulation results.

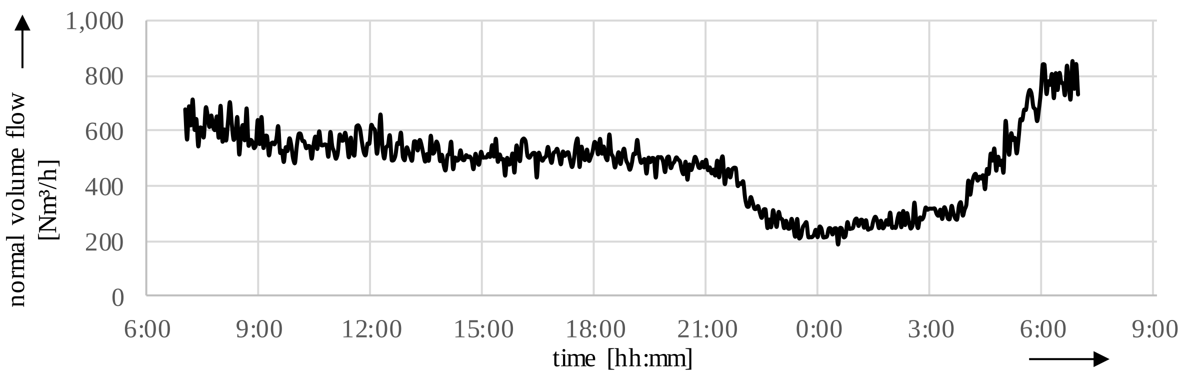

Figure 7: Normal volume flow over time for one day

Electrical power from the impulse turbine over a range of normal volume flow is presented as a scatter-plot in Figure 8. Note that every point can have a different rotational speed, which also can be different for the same normal volume flow due to controlling of the rotational speed in order to achieve an acceptable outlet temperature. The continuous line represents the result from the simulation for different rotational speeds. For the calculation of the electrical power, the internal power is multiplied with the generator efficiency which includes mechanical losses of the generator (bearing and sealing). It can be seen that up to a normal volume flow of 600 Nm³/h, the measured data are close to the simulated curve. Above a normal volume flow of 600 Nm³/h, less measured data are available, thus a wide distribution of the data is present due to control and transient processes. Furthermore, at a normal volume flow of 750 Nm³/h, flow inside the nozzle blades (GW) is choked. Therefore, the velocity triangle will not change essentially for higher normal volume flows. The absolute velocity at the nozzle outlet is equal to the speed of sound. Thus the specific internal work is nearly constant and the internal power is only dependent on the normal volume flow.

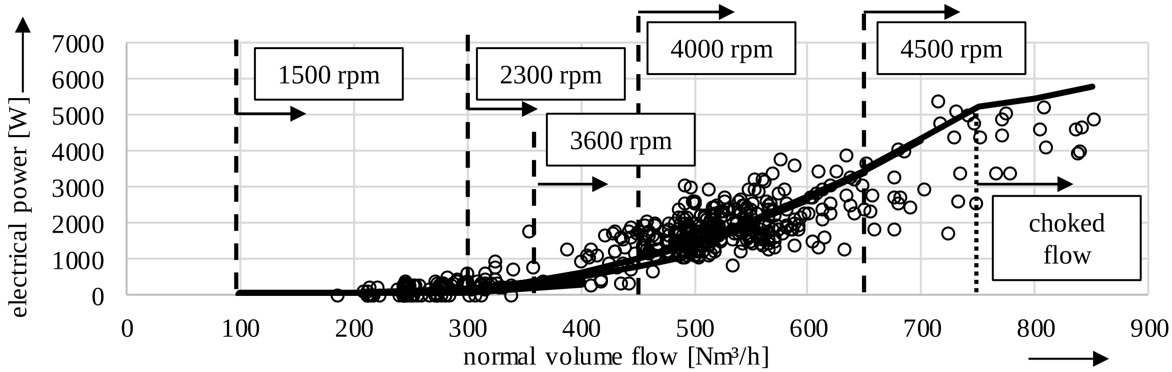

Figure 8: Electrical power depending on normal volume flow for different rotational speed

In Figure 9 the inlet pressure and the outlet temperature are shown dependent on normal volume flow. With increasing normal volume flow, the rotational speed increases as already shown in Figure 8. It can be seen that the inlet pressure of the turbine is higher in the experiment than the inlet pressure of simulation. Thus the pressure loss over the turbine is higher in the experiment than in the simulation. Possible reasons for additional pressure losses, which are not taken into account in the simulation, are changing cross sections between pipes (DN200) and turbine (DN400), the generator in the gas flow as a disturbance, and the flow straightener. From a normal volume of 750 Nm³/h, where the flow is choked, the pressure increases linearly with increasing volume flow. The outlet temperature measured directly behind the impeller is higher than that calculated using the simulation. However, the temperature pocket behind the impeller is installed on the opposite side of the admission, so a direct comparison is difficult. Also, the simulation is adiabatic, thus heat flow into the pipe are not taken into account. Furthermore, it is possible that the natural gas is heated slightly by the waste heat of the generator. In the range of the choked flow, temperature behind the impeller stays nearly constant.

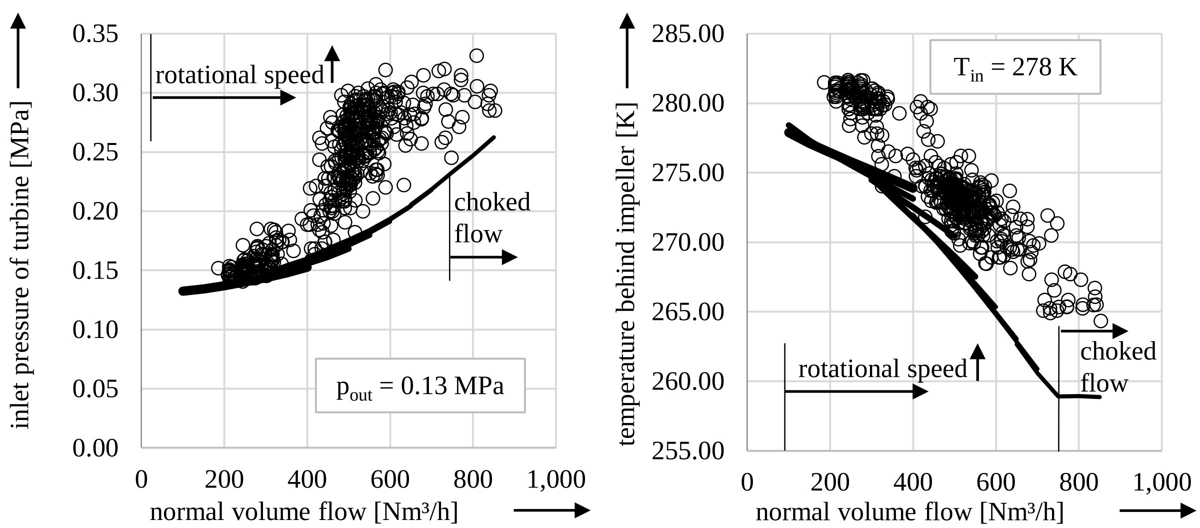

Figure 9: Left: Pressure difference over turbine depending on normal volume flow Right: temperature difference over turbine depending on normal volume flow

6. CONCLUSION AND OUTLOOK

A single stage axial impulse turbine module for natural gas expansion without additional heating equipment was designed, manufactured and tested in a natural gas pressure regulation station. Design and performance analysis of the turbine were performed using a one-dimensional mean line method with empirical models to predict losses.

Electrical power output, inlet pressure, and outlet temperature of the axial turbine with partial admission in a pressure regulation station were measured and compared with simulation results. For steady state operation points, the electrical power is close to the simulated curve. Inlet pressure is predicted higher in the simulations compared to experiment. Possible reasons are that in the simulations, pressure losses from the generator and flow straightener in the gas flow are not considered. The outlet temperature is predicted lower in the simulations compared to experiment. The essential reason for that is the location of the measurement point, which is on the opposite side of the impeller admission.
Our conclusion is that the mean-line method with empirical models is an acceptable and very fast approach for performance analysis. In future works, the disadvantage of high volume ranges in pressure regulation stations or natural gas storage facilities, where gas is expanded by outsourcing, can be considered. An improvement for the turbine to a maximum specific work for the whole volume flow range is a variable partial admission. A possible concept for realization of this approach is a combination of adaptive and passive change of partial admission depending on normal volume flow.

NOMENCLATURE

a	acceleration	(m/s²)	Y	total pressure loss coefficient	(-)
A	flow cross-section	(m²)	α	flow angle	(°)
b	blade	(-)	β	blade angle	(°)
c	absolute speed	(m/s)	η	efficiency	(-)
c	chord length	(m)	κ	isentropic coefficient	(-)
h	specific enthalpy	(J/kg)	**Subscript**		
h*	rothalpy	(J/kg)	bs	below the surface	
H	enthalpy	(J)	c	clearance	
Ma	Mach number	(-)	GW	guide wheel	
$\dot{m}$	mass flow	(kg/s)	h	height	
p	pressure	(Pa)	I	impeller	
P	power	(W)	1	inlet of blade row	
$\dot{Q}$	heat flow	(W)	in	inlet of the expansion machine	
r	radius	(m)	i	internal	
r	degree of reaction	(-)	s	isentropic	
s	specific entropy	(J/kg/K)	m	mean	
s	pitch	(-)	min	minimal	
T	temperature	(K)	2	outlet of blade row	
u	circumferential speed	(m/s)	out	outlet of the expansion machine	
v	specific volume	(m³/kg)	N	normal specification	
$\dot{V}$	volume flow	(m³/s)	th	theoretical	
w	relative speed	(m/s)	t	total	
w	specific work	(m²/s²)	w	wide	

REFERENCES

Lemmon E.W. (2013). *NIST Standard Reference Database 23*. Version 9.1 National Institute of Standards and Technology

Aungier R. (2005). *Turbine Aerodynamics*. New York: ASME Press.

Ainley, D. G. & Mathieson, G. C. R. (1951). A Method of Performance Estimation for Axial-Flow Turbine. *Aeronautical Research Council, R&M 2974*

Dunham, J. & Came, P. M. (1970). Improvements to the Ainley-Mathieson Method of Turbine Performance Prediction. *Journal of Engineering for Power,92*(3), 252-256

Kacker, S. C. & Okapuu, U. (1981). A Mean Line Prediction Method for Axial Flow Turbine Efficiency. *Journal of Engineering for Power, 104*(1), 111-119

ACKNOWLEDGEMENT

The work leading to these results has received in a joint project with innogy SE.